Int. J. Electrochem. Sci., 17 **(2022)** Article Number: 220630, doi: 10.20964/2022.06.19

International Journal of
ELECTROCHEMICAL
SCIENCE
www.electrochemsci.org

Short Communication

Effect of the Plating Time on Nickel Electroless Coating Properties Deposited on the Super Duplex Stainless Steel UNS S 32750

Dohyung Kim[1], *Kyungchung Kim*[2], *Wonsub Chung*[3,*] , *and Byung-Hyun Shin*[4,*]

[1] The Institute of Materials Technology, Pusan National University, Busan 46241, Republic of Korea
[2] School of Mechanical Engineering, Pusan National University, Busan 46241, Republic of Korea
[3] Eco-friendly Smart Ship Parts Technology Innovation Center, Pusan National University, Busan 46241, Republic of Korea
[4] Cold Rolling Production Engineering Team, Hyungdai steel, Dangjin-Si 31719, Republic of Korea
[*]E-mail: lemonhouse947@nate.com; wschung1@pusan.ac.kr

Received: 3 February 2022 / *Accepted:* 28 March 2022 / *Published:* 7 May 2022

Saw wires are used for Si wafer processing. That requires an excellent wear resistance and Ni-plating ability. Super duplex stainless steel (SDSS) contains 25 wt.% Cr, which endows it with high wear and corrosion resistance. The study about Ni plating on SDSS is required to use by saw wire because SDSS is a dual phase stainless steel composed of austenite and ferrite. However, not studies on Ni plated SDSS are available. In this study, electroless Ni plating was applied on the austenite of SDSS, thereby changing its electrochemical properties. Ni plated SDSS possesses an excellent wear resistance and an enhanced passivation layer, which improves its performance as a saw wire because of advanced passivation layer.

Keywords: Electrochemical properties; Super duplex stainless steel; Electroless Ni-plating; Potentiodynamic polarization curve; Passivation layer

1. INTRODUCTION

The steel alloyed with 12 wt.% Cr [1, 2] has an excellent wear resistance. These characteristics of STS make it suitable for use in saw wires. STS 304 is obtained after Ni and diamond plating, used in saw wires [3]. However, it has relatively low corrosion and wear resistance, causing it to easily corrode owing to the slip of diamond [5-8]. Therefore, adequate research on Ni plating is essential for developing anti-wear materials for saw wires.

In previous studies on Ni-plating, J. Cho analyzed the wear resistance of steel after subjecting it to Ni plating [9-11], whereas Y. Choi employed Ni plating in STS 304 and conducted a systematic analysis on the effects of different catalysts on this Ni plating reaction [12]. Although Ni plating has

been researched, there are no studies on the Ni plating on dual-phase stainless steel (austenite and ferrite), such as super duplex stainless steel (SDSS, 25 wt.% Cr) [13-17].

To incorporate SDSS into saw wires, an electrochemical reaction between Ni and the SDSS comprising austenite and ferrite is essential. Austenite and ferrite are important because they possess different mechanical and electrochemical properties. Ni plating begins with strike plating (Electroless plating), and an error in Ni plating will result in plating failure [12]. Therefore, to optimize the Ni plating conditions, it is necessary to analyze the surface conditions considering strike plating times.

In this study, based on the electroless Ni plating time, the microstructure of the SDSS and its surface roughness were analyzed via field emission scanning electron microscopy (FE-SEM) and atomic force microscopy (AFM), respectively. Its electrochemical properties were assessed through the open circuit potential (OCP) reactivity, while its electrochemical behavior was analyzed through a potentiodynamic polarization test. The reactivity of the plating was examined by electrochemical impedance spectroscopy (EIS), and the critical pitting temperature (CPT) was studied to observe the effect of the Ni plating on the SDSS.

2. EXPERIMENTAL

Duplex stainless steel is classified into four categories (Lean, standard, super, and hyper) based on the grade as per the pitting resistance number (PRE = wt. % Cr + 3.3 wt. % Mo + 16 wt. % N) [13].

Table 1. Chemical composition for electroless Ni plating of super duplex stainless steel UNS S 32750.

	C	**N**	**Mn**	**Ni**	**Cr**	**Mo**	**Cu**	**W**	**Fe**
UNS S 32750	0.01	0.27	0.8	6.8	25.0	3.8	0.2	0.02	Bal

Table 2. Electroless Ni plating condition (Electrolyte solution and condition) on super duplex stainless steel UNS S 32750.

Experimental condition	
Nickel chloride ($NiCl_2 * 6H_2O$)	240 g/L
Hydrogen chloride (HCl)	120 g/L
pH	4
Temperature	50 ℃
Stirring speed	350 rpm
Time	0 ~ 180 min

The material used in this study had 25 wt.% Cr and hence, was classified under the “super grade” with PRE 42. The chemical composition of SDSS is shown in Table 1. Ni chloride is main electrolyte solution and HCl is to keep going to pH 4. Temperature and Stirring reduce the concentration polarization.

The Ni plating on saw wires occurs in three steps; electroless Ni plating, electrolytic Ni plating, and electroless Ni plating. This study is conducted on strike plating, and the optimal conditions are listed in Table 2. The strike plating was carried out in an electrolyte solution composed of nickel chloride and

hydrochloric acid. The microstructure and electrochemical properties of the resultant product were analyzed as a function of the electroless plating time.

Following the electroless Ni plating and after polishing up to #2000, the microstructure and roughness were also measured as a function of the plating time via FE-SEM and AFM, respectively [15, 19].

The electrochemical properties were analyzed using a three electrode cell (a working electrode and specimens; a counter electrode and platinum mesh; and a reference electrode and saturated calomel electrode). The OCP, the potentiodynamic polarization, and EIS were recorded in a 3.5 wt.% NaCl electrolyte solution. The OCP was performed for 1 h, and the EIS was recorded at a frequency range of 10^{-1} to 10^{4} Hz. The potential polarization test was conducted over a voltage range of -0.6 V to 1.2 V at 0.167 mV intervals. The CPT is defined as the temperature at which the current exceeds 100 $\mu A/cm^2$ and remains so for longer than 1 min. This was evaluated in a 5.85 wt. % NaCl (1 mol) electrolyte solution with an applied potential of 700 mV and a temperature rate increase of 1 ºC/min.

3. RESULTS AND DISCUSSION

3.1. FE-SEM imaging as a function of strike plating time

Strike plating or electroless plating is most affected by plating time; therefore, it is important to have a uniform Ni-plating surface, which is the most influencing parameter in this case [12]. Fig. 1 shows the surface image of SDSS as a function of Ni-plating time [15].

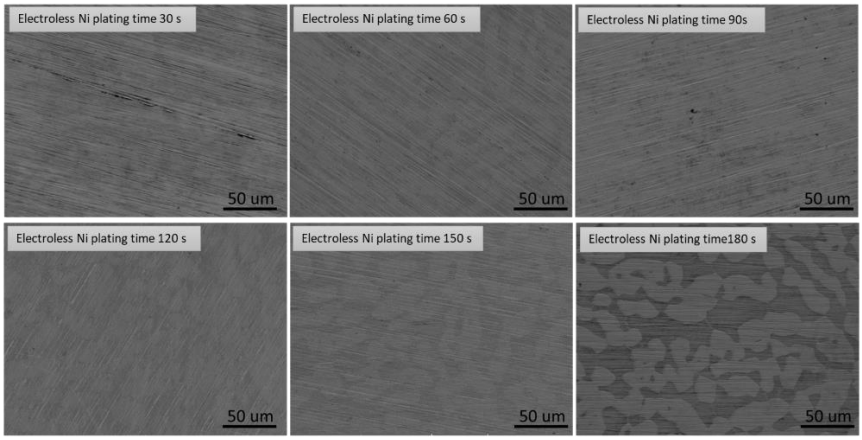

Figure 1. FE-SEM image of Ni electroless coating deposited on super duplex stainless steel UNS S 32750 at different plating time.

When the plating time exceeds 30 s, the traces of surface polishing can be confirmed from the image, but the traces of any subsequent polishing are diminished and the grain boundary between the austenite and ferrite is exposed.

To confirm the effects of the Ni plating compatibility on the SDSS, the grain boundaries between phases were measured via AFM, and the effects of strike plating were confirmed by the roughness [12].

The roughness is plotted against the electroless plating time. Although the surface roughness decreased initially, it increased subsequently as the grain boundary between austenite and ferrite appeared.

Nickel showed a difference in reactivity toward austenite and ferrite [11], which affected the strike plating and subsequent electrolytic plating.

3.2. Electrochemical properties as a function of strike plating time

The reactivity of the materials was measured as a function of the Ni plating time by its OCP. In Fig. 2, the effect of Ni-plating is plotted against the Ni plating time.

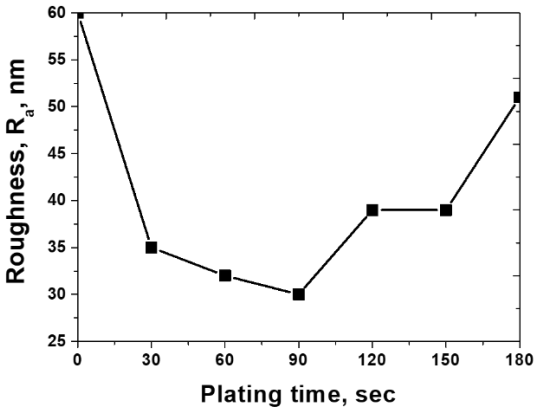

Time, s	R_a, nm
0	0.060
30	0.035
60	0.032
90	0.030
120	0.039
150	0.039
180	0.051

Figure 2. Roughness (nm) as function of a Ni plating time (Electroless Ni plating time) on super duplex stainless steel UNS S 32750.

Initially, the potential dipped, but as time advanced, the potential increased (# α to # β). Because the electroless Ni plating affects the reactivity of the SDSS, it is necessary to select the appropriate conditions for Ni electroless plating.

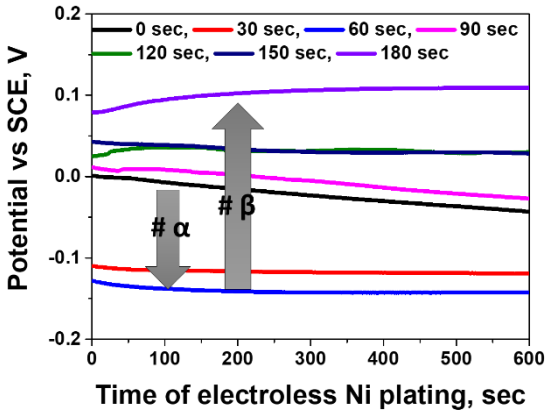

Figure 3. Open circuit potential curve (Potential with time) in 3.5 wt.% NaCl electrolyte solution as function of a electroless Ni plating time of super duplex stainless steel UNS S 32750.

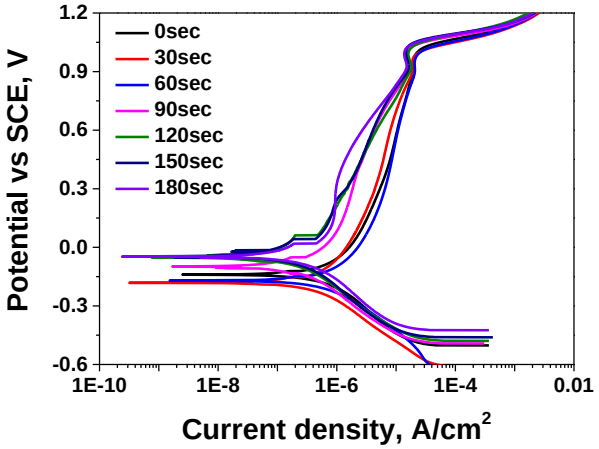

Figure 4. Potentiodynamic polarization curve of Ni electroless coatings (deposited on super duplex stainless steel UNS S 32750 at different plating time) in 3.5 wt.% NaCl electrolyte.

Since the potentiodynamic polarization test reveals the electrochemical behavior of the Ni-plated steel, it is possible to understand the characteristics of the Ni plated SDSS through various electrochemical analyses [13]. In Fig. 4 (Poteniodynamic polarization curve), the potential is shown as a function of current density, and the changes in values are shown in Table 3. In active polarization, E_{corr} and I_{corr} show the same trend as in the OCP results. After passivation, the pitting potential was different.

Table 3. Values of major point (E_{corr}, I_{corr}, and E_{pit}) as function of Ni plating time (Strike time) on potentiodynamic polarization curve of super duplex stainless steel UNS S32750

	0 s	**30 s**	**60 s**	**90 s**	**120 s**	**150 s**	**180 s**
E_{corr}	-0.134	-0.187	-0.183	-0.125	-0.033	-0.033	-0.033
I_{corr}	4×10^{-6}	5×10^{-6}	6×10^{-6}	1×10^{-6}	9×10^{-7}	9×10^{-7}	9×10^{-7}
E_{pit}	1.004	1.006	1.006	1.08	1.08	1.09	1.09

Through OCP and potentiodynamic polarization tests, it was confirmed that the strike Ni plating affected the electrochemical behavior of the SDSS [15]. Although the potential of nickel (-0.23 V) in the EMF series was lower than that of the SDSS, it played an important role in the strengthening the passivation layer after electroless Ni plating [12].

3.3. Discussion

As confirmed by the potentiodynamic polarization test, strike plating affects the passivation layer of the SDSS. However, the effect of Ni plating on the passivation layer of SDSS cannot be quantified. Therefore, EIS and CPT tests were performed to confirm the influence of the Ni plating on the passivation layer of SDSS [13, 15]. The corresponding results are shown in Fig. 5, respectively. The EIS

results confirm that the resistance increased after electroless Ni plating, but it was not confirmed that a new layer was formed.

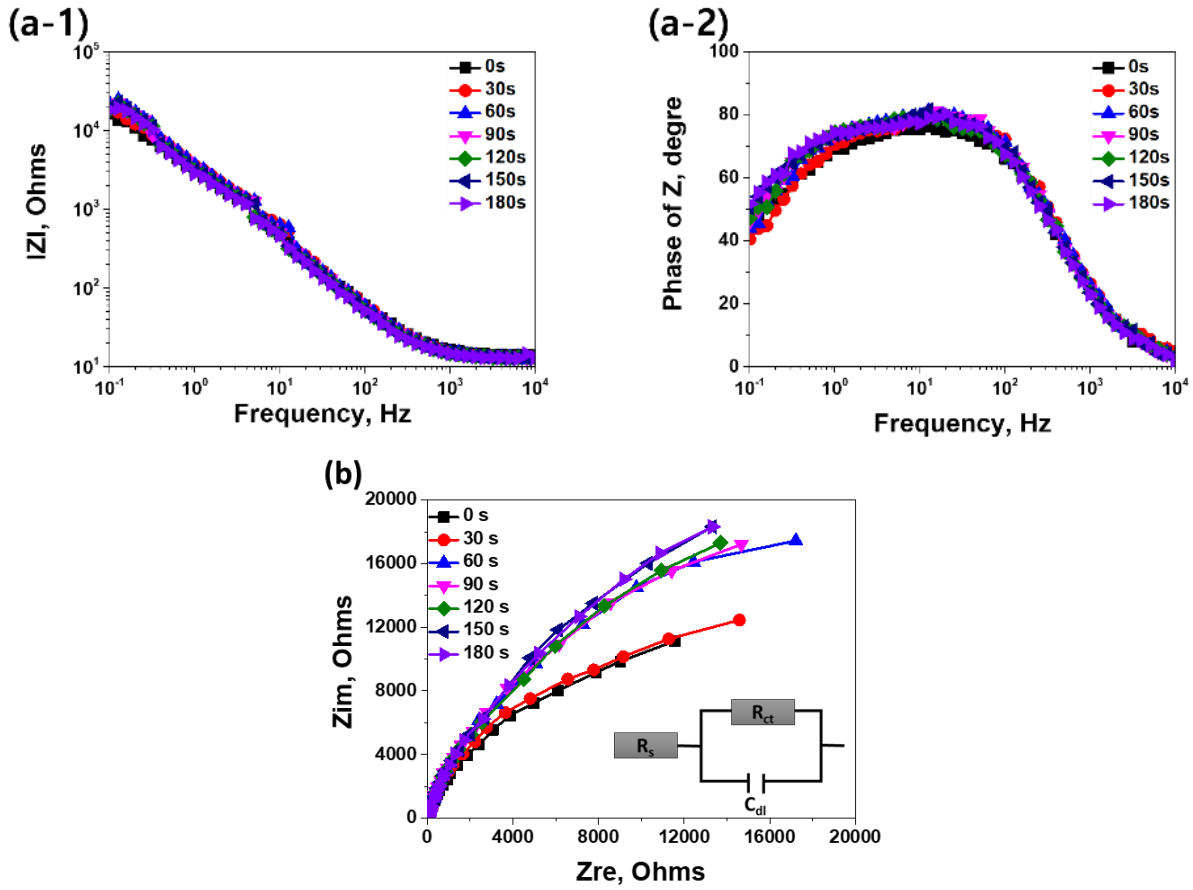

Figure 5. (a) Bode diagrams of electroless Ni plated super duplex stainless UNS S32750 in a 3.5 wt.% NaCl electrolyte solution (a-1) IZI as function of frequency (Ohms) and (a-2) Phase of Z (Ohms) as function of frequency (b) Nyquist diagram of UNS S32750 super duplex stainless steel in the conditions: electroless Ni plating time in a 3.5 wt.% NaCl solution.

Table 4. Values of resistance and CPE obtained for UNS S32750 with electroless Ni plating time.

Electroless Ni plating time	**R_s (Ohms)**	**CPE**		**R_p (Ohms)**
		C	n	
0 s	6.1	7.77×10^{-5}	0.82	372,260
60 s	6.0	7.56×10^{-5}	0.82	391,260
120 s	6.1	7.45×10^{-5}	0.81	412,870
180 s	6.0	7.31×10^{-5}	0.82	434,350

The electrochemical effect of the electroless Ni plated SDSS on the passivation layer was assessed by the potentiodynamic polarization tests and EIS. The Bode plot reveals a high phase (arc

degree) over a frequency range (10^{-1} ~ 10^{4}), a linear relationship with a slope close to 10^{-1} between IZI and frequency, and a phase decrease near I80°I at low frequencies, highlighting the highly capacitive passivation behavior typical of super duplex stainless steel [19]. The passivation behavior of SDSS is attributable to the considerably low passivation rate, and the equivalent circuit in Figure 5 is fitted to the EIS data to quantify the electrochemical parameters. The Ni plating layer on SDSS showed a form combined with the passivation layer of SDSS and advanced.

However, it is necessary to check its effect on pitting [20]. The CPT shows the effect on the pitting of SDSS. The CPT of the electroless Ni plated SDSS showed a difference as a function of the electroless Ni plating time and increased from 73 °C to 77 °C in Fig. 6. It was confirmed that Ni plating strengthens the passivation's layer of SDSS and increases its resistance to pitting.

The electroless Ni plating on SDSS had different reactivity toward austenite and ferrite [15]. In addition, electroless Ni plating on SDSS hastened the corrosion rate in the earlier stages but significantly increased the strength of the passivation layer from the 90 second mark.

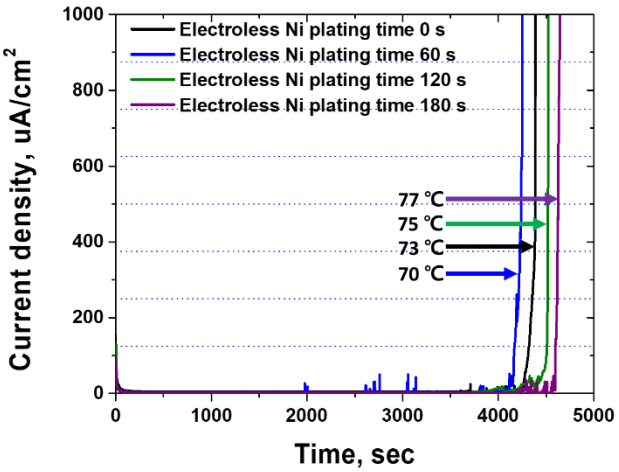

Figure 6. Current density as function of time (Critical pitting temperature curve) in 5.85 wt.% NaCl at 700 mV of electroless Ni plated SDSS.

4. CONCLUSION

The electroless Ni plating was performed on SDSS. Its microstructure was studied FE-SEM and AFM, whereas its electrochemical properties were analyzed with OCP, EIS, CPT, and electrostatic polarization tests. The following conclusions were drawn:

1) The electroless Ni plating on SDSS showed a difference in reactivity toward austenite and ferrite. As the plating time increased, the boundary between austenite and ferrite became sharper. The microstructure images recorded by AFM confirmed the effect of the Ni-plating silver phase on the SDSS.

2) The heterogeneous Ni plating layer decreased the potential of the SDSS. However, a uniform Ni plating increased the potential (E_{corr} and OCP) of the SDSS and increased the current density.

In addition, the nickel delayed the pitting (CPT, 73 °C to 77 °C) owing to the passivation layer (EIS) expansion.

3) Strike plating on SDSS showed a higher affinity toward the austenite and stabilized the passivation layer of the SDSS. The electroless Ni plated SDSS can be used to produce saw wires with a better performance than that of the base material.

ACKNOWLEDGEMENT
This work was supported by the National Research Foundation of Korea (NRF) grant, funded by the Korean government (MSIT) (No. 2020R1A5A8018822).
This work was supported by the Korea Institute for Advancement of Technology (KIAT) grant funded by the Korea Government (MOTIE) (P0002019, Human Resource Development Program for Industrial Innovation).

References

1. S. Jung, and K. Cho, *J. Kor. Inst. Surf. Eng*, 35, 1 (2002) 17.
2. S. Hoosain1, L Tshabalala, S. Skhosana, C. Freemantle, N. Mndebele1, *South African J. Ind. Eng*, 32, 3 (2021) dx.doi.org/10.7166/32-3-2661.
3. J. Cho, M. Yoo, S. Kang, *Met. Mater. Int*, 45 (2007) 514.
4. G. Gyawalia, D. Woob, S. Lee, *J. Kor. Inst. Surf. Eng*, 43, 4 (2010) 165.
5. E. Koehler, *Corrosion (Houston, Tx, U. S.),* 40 (1984) 5.
6. H. Leidheiser, *Jr. Corrosion*, 38 (1982) 374.
7. S. Yoo, Y. Kim, K. Chung, S. Baik, J. Kim, *Corros. Sci*., 59 (2012) 42.
8. P. Bommersbach, C. Alemany-Dumont, J.P. Millet and B. Normand, *Electrochim. Acta*, 51 (2005) 1076.
9. S. Moon, *J. Solid State Electr*., 18 (2014) 341.
10. C. E. Barchiche, E. Rocca, C. Juers, J. Hazan, and J. Steinmetz, *Electrochim. Acta*, 3 (2007) 417.
11. J. Liu, W. Yu, J. Zhang, S. Hu, L. You and G. Qiao, *Appl. Surf. Sci*., 256 (2010) 4729.
12. Y. Choi, D. Kim, K. Son, S. Lee, W. Chung, *Met. Mater. Int*, 21 (2015) 977.
13. J. Nilsson, and A. Wilson, *J. Mater. Sci. Technol*., 9 (1993) 545.
14. J. Nilsson, *J. Mater, Sci. Technol*., 8 (1992) 685.
15. B. Shin, J. Park, J. Jeon, S. Heo, and W. Chung, *Anti-Corros, Methods Mater*, 65 (2018) 492.
16. J. Kim, S. Choi, D. Park, and J. Lee, Mater Des, 65 (2015) 914.
17. B. Shin, D. Kim, S. Park, J. Park, M. Hwang, and W. Chung, *Anti-Corros, Methods Mater*, 66, 1 (2019) 61.
18. H. Ha, M. Jang, T. Lee, J. Moon, *Mater. Charact*, 106 (2015) 338.
19. D. Jiang,X.Gao, Y. Zhu, C. Hutchinson, A. Huang, Mater. Sci. Eng. A, 833 (2022) 142557.
20. P. Marcus, V. Maurice, H. Strehblow, *Corros. Sci,* 50 (2008) 2698.